Cell Transplant. Author manuscript; available in PMC 2016 May 02.

Published in final edited form as:

Cell Transplant. 2011 ; 20(7): 1065–1086. doi:10.3727/096368910X544906.

Schwann Cell Coculture Improves the Therapeutic Effect of Bone Marrow Stromal Cells on Recovery in Spinal Cord-Injured Mice

Xiaoyun Xu[*], **Nicole Geremia**[*], **Feng Bao**[*], **Anna Pniak**[*], **Melissa Rossoni**[*], and **Arthur Brown**[*,†]

[*]Spinal Cord Injury Team, BioTherapeutics Research Laboratories and Molecular Brain Research Group, Robarts Research Institute, The University of Western Ontario, London, Ontario, Canada

[†]Department of Anatomy and Cell Biology, The University of Western Ontario, London, Ontario, Canada

Abstract

Studies of bone marrow stromal cells (MSCs) transplanted into the spinal cord-injured rat give mixed results: some groups report improved locomotor recovery while others only demonstrate improved histological appearance of the lesion. These studies show no clear correlation between neurological improvements and MSC survival. We examined whether MSC survival in the injured spinal cord could be enhanced by closely matching donor and recipient mice for genetic background and marker gene expression and whether exposure of MSCs to a neural environment (Schwann cells) prior to transplantation would improve their survival or therapeutic effects. Mice underwent a clip compression spinal cord injury at the fourth thoracic level and cell transplantation 7 days later. Despite genetic matching of donors and recipients, MSC survival in the injured spinal cord was very poor (~1%). However, we noted improved locomotor recovery accompanied by improved histopathological appearance of the lesion in mice receiving MSC grafts. These mice had more white and gray matter sparing, laminin expression, Schwann cell infiltration, and preservation of neurofilament and 5-HT-positive fibers at and below the lesion. There was also decreased collagen and chondroitin sulphate proteoglycan deposition in the scar and macrophage activation in mice that received the MSC grafts. The Schwann cell cocultured MSCs had greater effects than untreated MSCs on all these indices of recovery. Analyses of chemokine and cytokine expression revealed that MSC/Schwann cell cocultures produced far less MCP-1 and IL-6 than MSCs or Schwann cells cultured alone. Thus, transplanted MSCs may improve recovery in spinal cord-injured mice through immunosuppressive effects that can be enhanced by a Schwann cell coculturing step. These results indicate that the temporary presence of MSCs in the injured cord is sufficient to alter the cascade of pathological events that normally occurs after spinal cord injury, generating a microenvironment that favors improved recovery.

Address correspondence to: Arthur Brown, Spinal Cord Injury Team, Robarts Research Institute, 100 Perth Drive, London, ON N6A 5K8, Canada. Tel: 519-931-5777, ext. 24308; Fax: 519-663-3789; abrown@robarts.ca.

Keywords

Bone marrow stromal cells (MSCs); Transplantation; Spinal cord injury; Anti-inflammatory; Stem cells

INTRODUCTION

Stem cell transplantation has been proposed to be a promising treatment for spinal cord injury (SCI). Theoretically, transplanted cells may contribute to repair after SCI by replacing lost neurons or glia or by producing factors that alter the injury site so as to enhance recovery and regeneration. Bone marrow, as a readily accessible source of both somatic stem cells, is an ideal source of donor cells for transplantation after SCI. In spinal cord-injured patients transplanted bone marrow-derived stem cells (MSCs) have been reported to be safe and potentially therapeutic (17). However, in spinal cord-injured patients as well as in patients with other neurodegenerative diseases clear mechanisms of action have not been elucidated for MSC transplantation nor has long-term survival or the fate of transplanted cells been adequately described (17,52). Studies of MSC transplantation in spinal cord-injured animals have also had difficulty demonstrating graft survival or mechanisms of action (50). Some of these studies show successful long-term engraftment of transplanted MSCs into the injured spinal cord (1,8,34–36,54,58,59) while others report that transplanted MSCs fail to engraft in significant numbers (less than a few percent of transplanted cells surviving >2 weeks) (9,24,25,40,41,46,56). A portion of the studies report improvements in locomotor function after MSC transplantation (8,9,24,25,34,41,54,56,58) whereas others do not (1,36,46). Interestingly, MSC survival in the spinal lesion does not appear to be necessary (41,56) or sufficient (1,36) for improved locomotor outcomes. However, even when improved locomotor recovery cannot be demonstrated, elements of the histopathological appearance of the lesion improve as shown by increased tissue sparing, altered extracellular matrix, and increased axonal growth at the injury site (1,35,36,46).

The emerging consensus appears to be that MSC transplantation may improve neurological outcomes and/or histopathological features of the lesion after SCI. However fundamental questions regarding the importance of graft survival, differentiation, and mechanisms of action still remain unanswered. Several studies using inbred rat strains (25) or immunosuppressants (40,41) failed to show good graft survival. This may reflect insufficient immunosuppression or, where inbred rat strains were used (25), that GFP expressed by donor cells may have been immunogenic (21). We predicted that using genetically matched EGFP transgenic donor and recipient mice would promote MSC survival after transplantation and that greater survival would correlate with improved neurological and histopathological outcomes. We also predicted that exposing MSCs to a neural environment (Schwann cells) prior to transplant might promote neural differentiation or compatibility and further increase their therapeutic effects. We herein report that despite using genetically matched EGFP donors and recipients, less than 3% of MSCs survived 2 weeks posttransplant and that by 5 weeks posttransplant the number of surviving MSCs was less than 1%. However, mice that received MSC transplants and, to a greater extent, those that

received Schwann cell cocultured MSCs (SMSCs), demonstrated improved neurological outcomes and beneficial changes in the lesion microenvironment.

MATERIALS AND METHODS

Cell Culture

All protocols for these experiments were approved by the University of Western Ontario Animal Care Committee in accordance with the policies established in the Guide to Care and Use of Experimental Animals prepared by the Canadian Council on Animal Care. Tg(ACTBEGFP)1Osb adult male mice, which express EGFP ubiquitously, were used to establish MSC cultures using the physical property of plastic adherence (15,18). This transgenic line of mice was selected as MSC donors because their MSCs can be traced after transplantation by their expression of EGFP. Once cells were 80% confluent, MSCs were passaged (1:3 dilution) with fresh medium. Flow cytometry was performed using antibodies raised against a battery of markers to characterize MSCs at passage 4, including c-kit, CD11b, CD31, CD34, CD45, and isotype controls.

Schwann cell cultures were established from C57B6 adult mice as described previously (60), and maintained separate from MSC cultures for 4–5 weeks at which time the cells were collected and counted with a hemocytometer. C57B6 mice were used as the source for the Schwann cells in the coculture experiments so that the EGFP-expressing MSCs could eventually be separated from the Schwann cells in these cultures by fluorescence-activated cell sorting (FACSvantage SE with Diva Option, BD Bioscience) based on EGFP expression in order to transplant SMSCs without contaminating Schwann cells. A 1:1 ratio of MSCs and Schwann cells was mixed in MSC culture medium and 5×10^5 total cells were plated into T-75-cm^2 flasks (BD Biosciences, Franklin Lakes, NJ), or 5,000 cells onto a coverglass in 12-well plates. MSCs were cocultured with Schwann cells for 1–10 days with medium changes every 48 h. $EGFP^+$ MSCs were immune stained with antibodies raised against the neural markers Tuj1 (Chemicon), GFAP (Calbiochem), or CC1 (Calbiochem) after 1, 3, 5, 7, and 10 days of Schwann cell coculture, respectively.

FACS of $EGFP^+$ MSCs From Schwann Cell Cocultures

After 5 days of coculture, the mixture of MSCs and Schwann cells was collected by trypsinization. The cell suspension was washed with 3% BSA in PBS, triturated, and passed through a 40-μm cell strainer to generate a single cell suspension. A culture of MSCs that had not undergone coculturing and a Schwann cell culture were treated with the same procedures to serve as positive and negative controls, respectively. EGFP-expressing SMSCs were isolated using FACS and collected into 100% FBS. The sorted SMSC EGFP-expressing cells were centrifuged at 1500 rpm for 5 min and resuspended at 10^7 cells/ml in saline prior to transplantation.

Mouse Model of SCI and Cell Transplantation

All injuries were performed on adult female C57B6-Kr15-EGFP mice that express EGFP in hair follicle bulge cells (38). These mice were selected to be the spinal cord-injured transplant recipients because they express EGFP on a C57B6 genetic background. EGFP in

these mice is expressed in hair follicles and thus we reasoned that EGFP expressed by transplanted MSCs or SMSCs would not be immunogenic in these recipients. Using an operating microscope, an 8.3 g force clip compression injury was made at the T4 segmental level as described previously (29,30,32). Transplantation was performed 7 days after SCI because MSC transplantation before this time has met with reduced graft survival (25). The dura was incised with the tip of an injection needle exposing the surface of the injured spinal cord. MSCs (3×10^4 cells/3 μl), SMSCs (3×10^4 cells/3 μl), or saline (3 μl) were injected into the cord at the lesion site using a spinal stereotaxic frame by means of a glass pipette (tip diameter 100 μm) configured to a 10-μl Hamilton syringe. In order to confirm that MSCs and SMSCs were delivered successfully into the injured cord, spinal cord sections collected from a small set of animals ($n = 4$ per group) 48 h posttransplantation were immunostained with an anti-EGFP antibody, and the signal visualized by a peroxidase-DAB reaction after a hematoxylin counterstain. A second set of animals (saline controls, MSCs, and SMSCs, $n = 12$ per group) underwent cardiac perfusion at 3 weeks postinjury and histological analyses for MSC and SMSC survival, macrophages, Schwann cells, chondroitin sulfate proteoglycans (CSPGs), neurofilament, and laminin. A third set of animals (saline controls, MSCs, and SMSCs, $n = 6$ per group) underwent locomotor testing for 6 weeks postinjury before cardiac perfusion and histological analyses for MSC and SMSC survival, myelin sparing, neuronal sparing, and collagen deposition (see Fig. 1 for experimental design).

Tissue Processing

At 48 h, 21 days, and 42 days after injury, mice were transcardially perfused with 4% paraformaldehyde in PBS. The C7–T10 vertebral segments, which included the site of the compression injury, were removed and processed for cryosectioning and immunohistochemistry. All sections were cut at a thickness of 16 μm. Sections spanning the injury sites were selected for analyses (Table 1). The maximum distance rostral and caudal to the injury investigated for pathology was determined by the distance from the lesion at which a particular pathological feature returned to baseline levels. The number of sections analyzed reflected the section-to-section variability (the greater the variability the more sections analyzed) to avoid a sampling bias.

Immunohistochemistry

Slides were incubated with the appropriate dilutions of primary antibodies in a humidified chamber at 4°C overnight. The list of primary and secondary antibodies used and their dilutions is provided in Table 2. The immunostained sections were examined using an Olympus epifluorescence microscope (BX51) and/or a Carl Zeiss confocal microscope (LSM 510 Meta) with an Argon-HeNel laser.

MSC and SMSC Survival After Transplantation

MSC and SMSC survival was quantified using spinal cord sections collected at 14 and 35 days after transplantation, respectively. Twenty-five sections from the area of cord 2 mm rostral and 2 mm caudal to the lesion epicenter representing one tenth of the total spinal cord volume in this segment were collected at a minimum of 32 μm apart from MSC- and SMSC-treated animals. The sections were stained with an anti-EGFP antibody, and the signal

visualized by a peroxidase-DAB reaction and hematoxylin counterstain. Y chromosome painting for engrafted MSC was also performed on adjacent sections using fluorescent in situ hybridization (FISH).

Assessment of Locomotor Function

Locomotor recovery of spinal cord-injured mice was assessed by two independent observers using the 9-point Basso mouse scale (BMS) from 1 day to 6 weeks after SCI (5). Testing was done once a week. Scores of the left and right hind limbs were averaged. The locomotor analysis and all other analyses detailed below were done blinded to the treatment the mice had received ($n = 6$ per group). Cumulative BMS scores were used to look for relationships between locomotor recovery and each of myelin sparing, neuronal sparing, and collagen deposition at the scar. Cumulative BMS scores were obtained by summing each animal's BMS score obtained over all trials. Cumulative BMS scores have been used by others (12) and avoids the problem of sample bias that may occur if only the final scores obtained on the last trial are used.

Measurement of White Matter Sparing

Transverse sections of spinal cord 6 weeks after injury were serially collected and mounted on glass slides. Ten sections from each cord, spanning approximately 1 mm in length across the lesion site, were stained with hematoxylin and eosin. Sections demonstrating the most severe disruption of normal white and gray matter architecture were considered to mark the position of the lesion epicenter in that animal. Nine sections at 250-μm intervals were processed for solochrome cyanin staining to identify the residual blue-stained white matter between the lesion epicenter and 1.5 mm rostral and caudal to the epicenter, respectively. Ratios of the stained area to the total area of the spinal cord section (per area measurements) were measured using ImagePro Plus software (Media Cybernectic, Silver Spring, MD). Because of the frequent distortion of the cord by scar and the compression at and near the lesion, white matter (per area) of sections from relatively intact cord at 2 mm caudal to the lesion epicenter in the same animal was also quantified and used to normalize the white matter areas closer to the lesion. The normalized per area values of white matter sparing were compared among three groups of animals and reported.

Measurement of the Collagen Deposition

Seven sections, each section separated by 160 μm, were processed for Masson's trichrome staining (Sigma, St. Louis, MO). Briefly, the sections were incubated in preheated Bouin's solution at 56°C for 15 min. Nuclei were stained black with Weigert's iron hematoxylin for 1 min at room temperature, and cytoplasm was then stained with Beibrich scarlet-acid fuchsin. After treatment with phosphotungstic and phosphomolybdic acid, collagen was demonstrated by staining with aniline blue. The blue-stained area was measured using ImagePro Plus Software and expressed as a percentage of the cross-sectional area of the same spinal cord section.

Assessment of Neuronal Sparing

NeuN-positive neurons within the lesion site were quantified 6 weeks after injury. Transverse sections were serially collected within 1.5 mm rostral and 1.5 mm caudal to the lesion epicenters at intervals of 80 μm and stained with an anti-NeuN antibody and an Alexa Fluor 594-conjugated secondary antibody. The number of NeuN-expressing cells was counted using ImagePro Plus software. Three continuous sections with the greatest loss of neurons defined the position of the lesion epicenter. Six sections 80 μm apart spanning the distance from the epicenter to ~0.5 mm rostral were stained for NeuN expression, and the number of immunoreactive cells averaged and normalized to the numbers of neurons from relatively intact spinal cord sections from the same animal. A second and third set of six sections 80 μm apart were likewise evaluated for NeuN expression between 0.5–1.0 mm and 1.0–1.5 mm from the lesion epicenter. The same process was repeated for spinal cord regions caudal to the lesion epicenters.

Analysis of CSPG, NF200, Laminin, and p75 Immunoreactivity

Immunohistochemistry to detect CSPG, neurofilament, laminin, and p75 was performed on four to six serial-collected longitudinal sections spaced 32 μm apart from the control, MSC, and SMSC transplant recipients 3 weeks postinjury. Immunostaining for CSPGs was done using CS56, an antibody that recognizes the terminal portions of chondroitin sulfate-4 or -6 side chains and thus detects a variety of CSPGs (3,13). For laminin and p75 immunoreactivity, one digital image per cord was taken across the lesion site, with a 10× objective. The signal intensity of CS56 and anti-NF200 immunostaining was reduced relative to that of the anti-laminin and p75 immunostaining, necessitating the use of higher magnification for microscopic examination. To quantify the area of immunoreactivity for CS56 and NF200, two equal-sized digital images were taken from each cord, using a 20× objective under identical illumination and exposure settings. One image was rostral and the other caudal to the lesion epicenter. Both images represented the highest intensity of CS56 or NF200 immunoreactivity in that area of the cord. Using the ImagePro Plus software, the digital images were imported as an 8-bit grayscale image and its meninges were trimmed off to eliminate nonspecific labeling. The threshold for positive signal was set at 75 in the histogram (0–225), which eliminated background staining. The number of pixels above the threshold was calculated, averaged with those of the same treatment group, and reported.

Density of Macrophages/Active Microglia at the Lesion Site

Twenty-one days after SCI, transverse sections were serially collected within the area of cord 1.0 mm rostral and 1.0 mm caudal to the lesion epicenters. One set of 25 sections at intervals of 80 μm was stained with an anti-Mac-1 antibody and followed by hematoxylin counterstain. The density of Mac-1-expressing cells of each section was calculated as numbers of Mac-1-positive cells/area of the section multiplied by the thickness of the section.

Cytometric Bead Array (CBA) Assay

The BD™ CBA mouse inflammation kit (BD Bioscience) was used to quantitatively measure interleukin-6 (IL-6), IL-10, monocytes chemoattractant protein-1 (MCP-1), interferon-γ

(INF-γ), tumor necrosis factor (TNF), and IL-12p70 protein levels in the supernatant collected from MSC culture, Schwann cell culture, and after 1, 3, 5, and 7 days of MSC–Schwann cell coculture, respectively. The assays were performed according to the manufacturer's instruction ($n = 4$). Briefly, six bead populations with distinct fluorescence intensities were coated with capture antibodies specific for IL-6, IL-10, MCP-1, INF-γ, TNF, and IL-12p70 protein; PE-conjugated detection antibodies and test samples were incubated together to form sandwich complexes. Standards provided with the kit were appropriately diluted and used in parallel to samples for preparation of the standard curves. Each supernatant sample (25 μl) was diluted at 1:2 with the assay diluents and added to 50 μl of capture beads mixture and 50 μl of detector Ab-PE. After incubating for 2 h at room temperature, the mixture was washed and analyzed using flow cytometry and the FCAP Assay software.

Y Chromosome Painting for Engrafted MSC Detection

Cryostat spinal cord sections (16 μm) collected 21 days after SCI were used for detection of engrafted male MSCs in the spinal cord-injured female recipients. The sections were first treated with 0.2N HCl for 30 min and incubated with sodium thiocyanate for 30 min at 80°C. The sections were digested with 1 mg/ml proteinase K (Invitrogen) for 45 min at 37°C and dehydrated through graded alcohols. The biotin-labeled mouse Y chromosome probes were denatured at 37°C for 43 min (Cambio, Dry Drayton, UK) before applying them to the sections. The slides were denatured at 75°C for 6 min, then hybridized with the Y chromosome probe for 20 h at 37°C. After hybridization, slides were washed in a 45°C water bath first in 1:1 formamide/1× SSC, then 1× SSC, and 1× SSC + 0.05% Tween 20. After washing, the Y chromosome signal was detected with an Avidin-Texas Red conjugate. Male mouse spinal cord sections served as positive controls.

Statistical Analysis

Mean values are expressed ±SE. Statistical analyses were performed using GB-STAT software. The MSC engraftment data and neuronal differentiation data were evaluated by Student's *t*-tests. Data for locomotor recovery, myelin sparing, collagen deposition, and Mac-1-positive cell density were analyzed by a two-way repeated measures ANOVA, with a Neuman-Keuls posttest. Data for area of CS56, NF200, laminin, p75 immunoreactivity, and CBA assay were analyzed by a one-way ANOVA with a Neuman-Keuls posttest. Correlations between cumulative BMS scores and myelin sparing, neuronal sparing, or area of collagenous scar were calculated using a single regression analysis. Differences were considered statistically significant if $p < 0.05$.

RESULTS

In Vitro Differentiation of MSCs

Five independent cultures of MSCs were isolated from the bone marrow of ACTB-EGFP transgenic adult male mice. Flow cytometry was used to characterize MSC cultures at passages 4–6. MSCs in culture did not express the stem cell marker c-kit, or markers of the hematopoietic (CD34, CD45, or CD11b) or endothelial (CD31) cell lineages (data not shown). The colony-forming unit-fibroblast (CFU-F) assay was used as a functional method

to quantify mesenchymal stem and progenitor cells in mouse bone marrow. The frequency of fibroblast-like colonies from each mouse bone marrow sample was about 0.0008–0.0018% ($n = 4$). To test the prediction that exposing MSCs to a neural environment prior to transplantation would increase the frequency of MSC neural differentiation in the injured spinal cord we cocultured the EGFP-expressing MSCs with wild-type (nontransgenic) Schwann cells prior to transplantation. Passage 4 MSCs were cultured with Schwann cells and then immunostained for EGFP expression and markers of neural differentiation after 1, 3, 5, 7, and 10 days of coculturing. A small percentage (~6%) of MSC not cocultured with Schwann cells was found to express the neuronal marker Tuj1 (β-III tubulin), but not GFAP or CC1, markers of astrocytes and oligodendrocytes, respectively (Fig. 2A–C). Five days after coculturing with Schwann cells, 13 ± 5.6% of MSC were immune positive for β-III tubulin, 13 ± 3.5% for GFAP, and 15 ± 2.7% positive for CC1 (Fig. 2D–F). Five days of Schwann cell coculturing was selected as the optimum time to collect MSCs for transplantation as all three neural markers showed the highest frequency of expression at this time point (Fig. 2G). EGFP-expressing SMSCs were isolated from the Schwann cells to 99% purity using FACS. Schwann cells maintained their characteristic morphology and were positive for S-100 during the coculture period.

MSC Transplants Survived Only Temporarily in the Spinal Lesion

K15-EGFP mice received a clip compression injury at the fourth thoracic (T4) segment of the spinal cord. K15-EGFP mice express EGFP in hair follicle stem cells. One week after injury animals received an intraspinal injection of either saline (3 μl), or EGFP-expressing MSCs (MSCs 3×10^4/3 μl) or Schwann cells cocultured EGFP-expressing MSCs (SMSCs, 3×10^4/3 μl). Immunohistochemistry using anti-GFP antibody revealed a total absence of GFP-expressing cells in the injured spinal cords of K15-EGFP control mice (Fig. 3A), demonstrating that recipient EGFP-expressing skin stem cells do not migrate to the injured spinal cord and that EGFP expression could be used to accurately track MSCs and SMSCs in mice after transplantation. Successful delivery of the MSCs and SMSCs into the lesion epicenter was verified by anti-EGFP immunostaining spinal cord sections from a subset of animals sacrificed at 48 h posttransplantation (Fig. 3B). The engrafted cells, mostly found at or close to the lesion epicenter, displayed robust EGFP expression and demonstrated as the typical MSC spindle shape.

Three and 6 weeks post-SCI MSC and SMSC engraftment was evaluated in sections by their EGFP expression. The majority of the MSCs and SMSCs were located at the interface between the lesion epicenter and spared neural tissue (Fig. 3C). The normal demarcation of white and gray matter was absent at the lesion epicenters, which were filled with inflammatory cells (Fig. 3D). Transplanted cells displayed robust EGFP expression that filled the cells as detected by both fluorescent and DAB immunostaining (Fig. 3C, E, F). The number of MSCs and SMSCs within a 4-mm section of cord surrounding the epicenter at 2 weeks posttransplant was 970 ± 240 and 1210 ± 280, respectively. At 6 weeks posttransplant the number of surviving MSCs and SMSCs in the spinal lesions fell to 410 ± 30 and 230 ± 30, respectively (Fig. 3F). To discount the possibility that MSCs and SMSCs were not detected because of reduced transgene expression, we used Y chromosome in situ hybridization to detect the male donor cells in the female recipients. This analysis

demonstrated comparable numbers of Y chromosome-positive cells and EGFP-expressing cells in the lesions of animals receiving the MSC grafts and that, where present, they coincided spatially in directly adjacent serial sections (Fig. 3G, H).

MSC and SMSC Transplantation Improved Locomotor Recovery

The 8.3 g clip compression injury was severe and in all mice caused a flaccid paralysis and little or no hind limb movement during the first week postinjury. Saline, MSCs, or SMSCs (Schwann cells were removed by cell sorting prior to injection) was administered 7 days postinjury. Locomotor recovery in the saline-treated mice was marginal with animals in this group reaching a maximum BMS score of 1 ± 0.47, indicating that these animals were only capable of slight ankle movement 6 weeks postinjury (Fig. 4). MSC-treated mice achieved a maximum BMS score of 1.9 ± 0.53, indicating extensive ankle movement. SMSC-treated mice recovered extensive ankle movement and many in this group also demonstrated plantar placement (average BMS score of 2.5 ± 0.83). Chi-square analysis revealed a higher observed frequency of plantar placement (4/6) in the SMSC group versus saline controls (0/6) 6 weeks postinjury ($\chi^2 = 6.0$, $p < 0.02$). Repeated measures ANOVA revealed improved locomotor recovery in MSC- and SMSC-treated mice as indicated by the significant group × time interaction ($p = 0.004$). Locomotor improvements were statistically significant between SMSC- and saline-treated mice as early as 3 weeks postinjury and between MSC- and saline-treated mice by 4 weeks postinjury. At 3 weeks postinjury SMSC-treated mice demonstrated statistically significant improved locomotor recovery compared to MSC-treated mice, although this difference was not maintained at later time points.

SMSC Transplantation Promoted Myelin Sparing

Solochrome cyanine staining of histological sections spanning 2 mm from the lesion epicenters of saline-, MSC-, and SMSC-treated mice was analyzed for the presence of white matter 6 weeks postinjury. The area of white matter per section was measured using ImagePro software to quantify the amount of blue-stained myelin. This analysis revealed increased myelin sparing in SMSC-treated mice (group × distance from the lesion, $p = 0.008$). In control and treatment groups the injury resulted in almost complete loss of the white matter at the epicenter (Fig. 5A–C). Near the lesion center, at 0.25 mm rostral and caudal to the epicenter, myelin was detected in small patches that constituted a small percentage of the normalized cross-sectional area of the cord in both control and treated mice. At 0.5 mm (Fig 5D–I) and 0.75 mm (Fig. 5J) rostral and caudal to the epicenter, SMSC-treated mice had substantially more visible myelin, compared to MSC-treated mice and saline control mice (Fig. 5D–I). At 1 mm from the injury site, the tissue retained much of its normal structure, and thus no significant difference in the amount of myelin staining was found between control and treated groups this distance from the lesion epicenter (Fig. 5J). Linear regression analysis revealed a significant correlation between cumulative BMS scores and myelin sparing 0.5 mm from the lesion epicenter ($r^2 = 0.84$) (Fig. 5K).

SMSC and MSC Transplantation Promoted Neuronal Sparing

Immunohistochemistry using an anti-NeuN antibody on histological sections spanning 3 mm centered on the lesion epicenters of saline-, MSC-, and SMSC-treated mice was used to assess neuronal sparing. The lesion epicenter, which extended about 0.5 mm, had a complete

loss of neurons in both ventral and dorsal horns. Neuronal survival adjacent to the lesion was significantly improved in SMSC-treated mice compared to either MSC-treated mice or saline controls (group × distance from lesion, $p < 0.0001$). At 0.5 mm rostral to the lesion center, 32 ± 4.8% of neurons survived in SMSC-treated mice, compared to 22 ± 7.2% in MSC-treated mice and 26 ± 5.8% in saline controls (Fig. 6A–C). At 1.0 mm rostral, 80 ± 4.1% of neurons survived in SMSC-treated mice, while only 55 ± 10.6% of neurons survived in MSC-treated and 55 ± 7.0% in saline-treated mice (Fig. 6D–F). At 1.5 mm rostral and caudal to the lesion epicenters neuronal loss was minimal in the all groups (neuronal survival rate >90%) (Fig. 6G–J). Caudal to the lesions a statistically significant increase in neuronal survival was evident in SMSC-treated mice at 1.0 mm from the lesion epicenter and in both MSC- and SMSC-treated mice relative to saline controls at 0.5 mm caudal to the lesion epicenter (Fig. 6J). Linear regression analysis showed significant correlation between cumulative BMS scores and neuronal sparing 1.0 mm from the lesion epicenter ($r^2 = 0.80$) (Fig. 6K).

SMSC Transplantation Significantly Reduced the Collagen Deposition at the Lesion Site

The histopathological response in mice following SCI is characterized by secondary lesion sites that are filled with macrophages and fibroblasts embedded in a well-vascularized collagenous stroma (27,37). The collagenous scar has been implicated as an obstacle to axonal regeneration in brain and spinal cord injury (22,48). At 6 weeks after SCI, Masson's trichrome staining demonstrated significant decreases in collagen deposition (blue) in the injured spinal cord of SMSC-treated mice (group × distance from lesion, $p = 0.04$). At the epicenter of SMSC-treated mice 31 ± 6.7% of the spinal cord cross-sectional area was occupied by collagen compared to 42 ± 8.7% and 40 ± 10.9% in MSC- and saline-treated mice, respectively (Fig. 7A–C). At 0.16 mm rostral and caudal to the epicenter, about 20% of the spinal cord cross-sectional area was occupied by collagen in SMSC-treated mice, compared to 30% in MSC- and saline-treated mice (Fig. 7D–I). At 0.5 mm rostral and caudal to the lesion epicenters, the amount of collagen deposition became minimal (<10%) in treated and control groups (Fig. 7J). Linear regression analyses indicated an inverse correlation between cumulative BMS scores and collagen staining at 0.16 mm from the lesion epicenter ($r^2 = 0.43$) (Fig. 7K).

MSC and SMSC Transplantation Decreases CSPG and Increases Laminin in the Scar

The absence of axonal regeneration after SCI has been attributed, in part, to axon-repelling CSPGs in the scar produced in response to the injury (13). However, some components of the scar, namely laminin and fibronectin, promote axonal growth (10,14,51,55). Thus, we evaluated CSPG and laminin expression in the lesions of treated and untreated mice 3 weeks postinjury using an antibody, CS56, that recognizes many different CSPGs (3,13) and an anti-laminin antibody. The 3-week postinjury time point was chosen for this analysis because BMS scores begin to improve at this time. In all groups, the intensity of CSPG immunoreactivity was most pronounced in the penumbra adjacent to the lesion epicenter (Fig. 8A–C). The area of CSPG immunoreactivity was substantially reduced in MSC- and SMSC-treated mice compared to saline controls (Fig. 8A–D). MSC-treated mice showed an increase in the area of laminin immunoreactivity surrounding the lesion relative to controls,

and SMSC-treated mice showed increased laminin expression surrounding the lesion compared to both MSC-treated mice and controls (Fig. 8E–H).

The reductions in collagen and CSPG and increase in laminin expression in MSC- and SMSC-treated mice led to the prediction that MSC- and SMSC-treated mice would demonstrate greater amounts of axonal growth in their lesions than saline controls. To test this prediction we performed immunohistochemistry on sections through the lesion epicenters in all three groups of mice using an anti-neurofilament (NF200) antibody. The area of NF200 immunoreacitivity was increased in the penumbra in MSC- and SMSC-treated mice (Fig. 8I–L). There was a near total absence of NF2000 immunostaining in the epicenter of the lesion in saline- and MSC-treated mice, whereas NF200 staining was present in the core of the lesion in SMSC-treated mice (Fig. 8, insets i–k).

Identification of Serotonergic Axons Caudal to the Lesion After MSC or SMSC Treatment

Descending serotonergic (5-HT-positive) axons provide excitatory input to motor neurons and the loss of these inputs has been correlated to locomotor dysfunction (44). We evaluated serotonergic fiber density in longitudinal sections spanning the lesion epicenters in saline controls and MSC- and SMSC-treated mice 3 weeks after SCI. In all groups of mice, a dense accumulation of 5-HT-positive axons occurred rostral to the lesion (Fig. 9A–D). 5-HT immunoreactivity ceased abruptly at the boundary of the lesion epicenters with virtually no 5-HT immunoreactivity observed in the epicenters of the saline control group and MSC-treated group. However 5-HT-positive fibers were found along the subpial rim of the cord, on the lateral edge of MSC- and SMSC-treated lesions (Fig. 9E, F), as well as in the lesion epicenters in SMSC-treated mice (Fig. 9F). 5-HT-positive fibers were also distributed caudal to the lesion in MSC- and SMSC-treated mice (Fig. 9H, I). 5-HT-positive fibers were not seen at the subpial rim or in the regions caudal to the lesion in saline controls.

SMSCs Led to Robust Recruitment of Endogenous Schwann Cells Into the Injury Site

MSCs transplanted into the injured spinal cord have been shown to increase Schwann cell infiltration of the injury sites (24,35,36). We evaluated Schwann cell infiltration of the injury sites in saline controls and MSC-and SMSC-treated mice using immunohistochemistry and an anti-p75 antibody. Schwann cells were present in the injured spinal cords in all three groups. The area of p75 immunoreactivity was used to assess the relative numbers of Schwann cells in the lesions of saline controls and MSC- and SMSC-treated mice. This analysis revealed that a greater number of Schwann cells infiltrated the lesions in SMSC-treated animals compared to MSC-treated animals or controls (Fig. 10A–D). Double immunostaining with anti-p75 antibodies and antibodies raised against the peripheral myelin marker P0 demonstrated that some Schwann cells produced myelin and may have participated in axon remyelination (Fig. 10E). Since Schwann cells have been shown to produce laminin in the injured spinal cord and the MSC- and SMSC-treated mice demonstrated higher levels of both Schwann cell infiltration and laminin immunoreactivity in their lesions, we immunostained serial sections with anti-p75 and anti-laminin antibodies to investigate the spatial distribution of laminin relative to the Schwann cell population. The spatial overlap of the anti-p75 and anti-laminin immunohistochemistry suggests that Schwann cells may be a source of laminin in these lesions (Fig. 10F–H).

MSC/SMSC Transplantation Decreases the Number of Mac-1- Positive Macrophages at the Lesion

The reported immunomodulatory effects of MSC transplants (39,53) and the altered scar deposition in our SMSC-treated mice led us to evaluate the macrophage population in the lesions in the treated and untreated mice. We used Mac-1 antibody to immunostain macrophages and microglia in the injured spinal cord 3 weeks after injury. The majority of Mac-1-positive cells were found at or near the injury epicenter and decreased distally (Fig. 11A–F). The density of Mac-1^+ cells was much lower in MSC-treated (2526 ± 471/mm^3) or SMSC-treated animals (2011 ±295/mm^3) compared to saline controls (5442 ± 532/mm^3) at the lesion epicenters (group × distance from the lesion, $p < 0.0001$). There were also far fewer Mac-1^+ cells 0.5 mm rostral and caudal to the lesion epicenters in MSC- and SMSC-treated mice compared to saline controls (Fig. 11G).

Schwann Cell Coculturing Alters MSC Chemokine Production

The greater reduction in macrophages at the lesions of SMSC-treated compared to MSC-treated mice suggested that the SMSCs and MSCs may differ in their chemokine or cytokine expression profiles. To measure the release of cytokines/chemokines by MSCs, before and after coculturing with Schwann cells, we measured IL-6, IL-10, MCP-1, INF-γ, TNF, and IL-12p70 protein levels in conditioned media from MSC cultures, Schwann cultures, and Schwann cell-MSC cocultures after 1, 3, 5, and 7 days, using the mouse inflammation CBA assay. Standard curves from 0 to 2500 pg/ml for each cytokine were generated according to the manufacturer's recommendations and used to calculate the level of each cytokine in the conditioned media (Fig. 12A, B). Only IL-6 and MCP-1 were detectable in MSC and Schwann cell culture medium (Fig. 12C, D). A significant decrease in both IL-6 and MCP-1 were demonstrated in the Schwann cell–MSC cocultures at all time points evaluated (Fig. 12E, F).

DISCUSSION

We hypothesized that by matching donor and recipient mice for genetic background and MSC maker gene expression (EGFP) we would maximize MSC survival in the injured spinal cord. However, only a few percent of transplanted, syngeneic MSCs survived 2 weeks post-transplant in the injured cord. What might explain the long-term survival of MSCs as claimed in some cases of MSC transplantation into the spinal cord-injured rat? One explanation may be that in those studies cells were injected into, or took up residence in, the developing cyst that forms in the injured rat spinal cord (1,35, 36,54,58,59). The cyst may create a microenvironment that protects MSC from inflammation or it may provide a confined space that allows MSC-produced growth factors to reach critical levels to support their own survival. Mouse spinal cords do not develop large cystic cavities after injury as do rats (7,28), and MSC survival is poor in the rat when transplants are performed early after injury, before a cyst may develop (56).

MSC- and SMSC-treated mice demonstrated statistically significant improvements in their locomotor recovery. Animals in the saline control group achieved an average BMS of 1 ± 0.47, indicating that these animals were only capable of slight ankle movement 6 weeks

postinjury. SMSC-treated mice demonstrated far better recovery with most animals in this group showing plantar placement by 6 weeks postinjury (average BMS score of 2.5 ±0.83). The small number of surviving transplanted cells suggests that cell replacement was not the mechanism through which MSCs and SMSCs improved outcomes in mice after SCI. Since MSC are known to have anti-inflammatory effects (39,53), we evaluated the possibility that the improved neurological outcomes could be attributed to increased neuroprotection or altered scar deposition in mice receiving MSC grafts. White matter sparing was increased in SMSC-treated mice and neuronal sparing was increased in both MSC- and SMSC-treated mice. Wound healing, scarring, and matrix deposition are ongoing processes that are also linked to the inflammatory response (20). The treated mice had less collagen scar as well as less CSPG and more laminin expression in their lesions. The amount of collagen scarring correlated negatively with locomotor recovery, as expected, given the well-known detrimental effects of scarring on axonal plasticity and regeneration. The decreased CSPG and increased laminin levels in treated mice led to the prediction that axonal growth might be increased in these animals (4,6,16,26,55). Changes in axonal growth around the lesion that correlated with the observed changes in matrix deposition were assessed by neurofilament immunoreactivity. Both MSC- and SMSC-treated mice had greater amounts of neurofilament staining in the penumbra rostral and caudal to the lesion. SMSC-treated mice also had increased amounts of neurofilament staining in their lesion epicenters. This evidence of increased structural plasticity around and within the lesion epicenters could account for the improved locomotor scores in MSC- and SMSC-treated mice as it confirms that the lesions in these mice permit or promote axon sprouting from spared axons that may underlie new circuitry transmitting supraspinal input past the lesion sites. In the severe injury model used in this study one might expect that recovery might be more dependent on local circuitry as opposed to descending supraspinal inputs. Improvements in the lesion microenvironment that promote axon sprouting might facilitate the formation of these circuits and or their function. It may be telling to note that the reports of improved locomotion in spinal cord-injured animals receiving MSC transplants tend to be those that use more severe injuries (25,41,56) as opposed to less severe ones (1,36).

The improved locomotor function in the treated mice could also be explained by increased sparing of supraspinal inputs that synapse below the level of the lesion. To investigate the possibility that spared supraspinal inputs may contribute to the locomotor recovery in these mice, we stained sections for 5-HT immunoreactivity as supraspinal serotonergic inputs to the ventral horn are critical to motor function after SCI (44). The strong 5-HT immunoreactivity at, and caudal to, the lesion epicenters in mice receiving MSC transplants contrasts with the absence of 5-HT staining in saline controls. Thus, increased BMS scores in treated mice may be due to combination of increased structural plasticity at the lesion and increased spared supraspinal serotoneregic inputs.

The MSC and SMSC treatments also changed the cellular component of the lesion microenvironment. In particular, lesions in both MSC- and SMSC-treated mice had fewer Mac-1^+ macrophages and more Schwann cells in their lesion epicenters than saline controls. The transplants may reduce the infiltration and activation of both the monocyte-derived macrophages and resident microglia. However, since monocyte-derived macrophages predominate at the lesion epicenter and their infiltration peaks between 7 and 14 days after

SCI in C57B6 mice (33), it is most likely that the MSCs and SMSCs reduced the number of monocyte-derived macrophages at the injury site. The decreased number of macrophages in the lesions of treated mice may account for some of the increase in white matter sparing observed, as others have reported increased white matter sparing after SCI by strategies that lower neutrophil and macrophage infiltration (19,43,45). The increased number of Schwann cells drawn into the lesions of mice that received MSC grafts may have contributed to the increase in laminin in these lesions as Schwann cells express laminin (31) and the distribution of laminin correlates spatially with the Schwann cell distribution in these mice. In addition to the production of laminin, increased Schwann cells in the treated mice may account for other improvements in recovery as Schwann cells may be a source of growth factors in the injured cord (36) and both endogenous Schwann cells and transplanted Schwann cells have been shown to improve recovery after SCI (23,49).

SCI triggers innate and adaptive immune responses that exacerbate the injury and increase tissue loss (2). Given the known suppressive effects of MSCs on innate and adaptive immunity, one possible explanation for the observed improved outcomes in MSC- and SMSC-treated spinal cord-injured mice is that the MSCs suppressed the immune response, resulting in greater tissue sparing, and an improved lesion environment for recovery (47,57). The greater positive effect of SMSCs compared to MSCs on neurological outcomes after SCI suggests that the Schwann cell coculturing step induced SMSCs to produce a different cytokine and/or chemokine profile when introduced into the injured spinal cord than that produced by MSCs without the coculturing step. While we did not evaluate cytokine or chemokine profiles of transplanted MSCs and SMSCs in vivo, we did demonstrate that MSC-Schwann cell cocultures produced 70% less IL-6 and MCP-1 relative to MSC cultures. Thus, the SMSC transplants may have performed better than the MSC transplants by virtue of having undergone a priming step, resulting in reduced expression of MCP-1 and IL-6 even before transplantation. MSC–Schwann cell cocultures also produced 90% less MCP-1 and IL-6 compared to Schwann cell cultures, suggesting that MSCs have the ability to reduce cytokine expression by Schwann cells. This effect of MSCs on Schwann cells in vitro suggests that MSCs and SMSCs may likewise lead to reduced levels of proinflammatory chemokines and cytokines in the injured spinal cord. Reduced levels of MCP-1, one of the key chemokines that regulate migration and infiltration of monocytes/macrophages (11), and IL-6, a proinflammatory cytokine (42), might account for the reduced levels of macrophages and immune-mediated secondary damage, respectively, in the injured spinal cords receiving the MSC and SMSC transplants.

We have demonstrated that the temporary survival of transplanted MSCs in the injured mouse spinal cord is sufficient to achieve improved locomotor recovery, histopathological evidence of neuroprotection, and changes in the lesion microenvironment that can enhance recovery and regeneration. We suggest that coculturing MSCs with Schwann cells likely enhances their immunosuppressive effects and that these cells thereby alter the cascade of destructive events that normally occur as a consequence of SCI resulting in greater neuroprotection and changes in the molecular and cellular make-up of the lesion microenvironment. This effect may be due to one or several factors produced by the transplanted cells. Since SMSCs outperform MSCs on every histopathological index of recovery, an investigation of differences in gene expression profiles in MSCs and SMSCs

should identify key molecular determinants that direct the healing process after SCI toward a more favorable outcome.

Acknowledgments

This work was supported in part by grants from the Canadian Institutes of Health Research (CIHR), The Ontario Research and Development Fund, and The Krembil Foundation (Toronto).

References

1. Ankeny DP, McTigue DM, Jakeman LB. Bone marrow transplants provide tissue protection and directional guidance for axons after contusive spinal cord injury in rats. Exp Neurol. 2004; 190(1): 17–31. [PubMed: 15473977]
2. Ankeny DP, Popovich PG. Mechanisms and implications of adaptive immune responses after traumatic spinal cord injury. Neuroscience. 2009; 158(3):1112–1121. [PubMed: 18674593]
3. Avnur Z, Geiger B. Immunocytochemical localization of native chondroitin-sulfate in tissues and cultured cells using specific monoclonal antibody. Cell. 1984; 38(3):811–822. [PubMed: 6435883]
4. Barritt AW, Davies M, Marchand F, Hartley R, Grist J, Yip P, McMahon SB, Bradbury EJ. Chondroitinase ABC promotes sprouting of intact and injured spinal systems after spinal cord injury. J Neurosci. 2006; 26(42):10856–10867. [PubMed: 17050723]
5. Basso DM, Fisher LC, Anderson AJ, Jakeman LB, McTigue DM, Popovich PG. Basso mouse scale for locomotion detects differences in recovery after spinal cord injury in five common mouse strains. J Neurotrauma. 2006; 23(5):635–659. [PubMed: 16689667]
6. Bradbury EJ, Moon LD, Popat RJ, King VR, Bennett GS, Patel PN, Fawcett JW, McMahon SB. Chondroitinase ABC promotes functional recovery after spinal cord injury. Nature. 2002; 416(6881):636–640. [PubMed: 11948352]
7. Brown A, Jacob JE. Genetic approaches to autonomic dysreflexia. Prog Brain Res. 2006; 152:299–313. [PubMed: 16198709]
8. Chopp M, Zhang XH, Li Y, Wang L, Chen J, Lu D, Lu M, Rosenblum M. Spinal cord injury in rat: Treatment with bone marrow stromal cell transplantation. Neuroreport. 2000; 11(13):3001–3005. [PubMed: 11006983]
9. Cizkova D, Rosocha J, Vanicky I, Jergova S, Cizek M. Transplants of human mesenchymal stem cells improve functional recovery after spinal cord injury in the rat. Cell Mol Neurobiol. 2006; 26(7–8):1167–1180. [PubMed: 16897366]
10. Costa S, Planchenault T, Charriere-Bertrand C, Mouchel Y, Fages C, Juliano S, Lefrancois T, Barlovatz-Meimon G, Tardy M. Astroglial permissivity for neuritic outgrowth in neuron-astrocyte cocultures depends on regulation of laminin bioavailability. Glia. 2002; 37(2):105–113. [PubMed: 11754209]
11. Deshmane SL, Kremlev S, Amini S, Sawaya BE. Monocyte chemoattractant protein-1 (MCP-1): An overview. J Interferon Cytokine Res. 2009; 29(6):313–326. [PubMed: 19441883]
12. Dijkstra S, Duis S, Pans IM, Lankhorst AJ, Hamers FP, Veldman H, Bar PR, Gispen WH, Joosten EA, Geisert EE Jr. Intraspinal administration of an antibody against CD81 enhances functional recovery and tissue sparing after experimental spinal cord injury. Exp Neurol. 2006; 202(1):57–66. [PubMed: 16806185]
13. Fawcett JW, Asher RA. The glial scar and central nervous system repair. Brain Res Bull. 1999; 49(6):377–391. [PubMed: 10483914]
14. Fok-Seang J, Smith-Thomas LC, Meiners S, Muir E, Du JS, Housden E, Johnson AR, Faissner A, Geller HM, Keynes RJ, Rogers JH, Fawcett JW. An analysis of astrocytic cell lines with different abilities to promote axon growth. Brain Res. 1995; 689(2):207–223. [PubMed: 7583324]
15. Friedenstein AJ. Marrow stromal fibroblasts. Calcif Tissue Int. 1995; 56(Suppl 1):S17.
16. Galtrey CM, Fawcett JW. The role of chondroitin sulfate proteoglycans in regeneration and plasticity in the central nervous system. Brain Res Rev. 2007; 54(1):1–18. [PubMed: 17222456]

17. Geffner LF, Santacruz P, Izurieta M, Flor L, Maldonado B, Auad AH, Montenegro X, Gonzalez R, Silva F. Administration of autologous bone marrow stem cells into spinal cord injury patients via multiple routes is safe and improves their quality of life: Comprehensive case studies. Cell Transplant. 2008; 17(12):1277–1293. [PubMed: 19364066]
18. Goshima J, Goldberg VM, Caplan AI. Osteogenic potential of culture-expanded rat marrow cells as assayed in vivo with porous calcium phosphate ceramic. Biomaterials. 1991; 12(2):253–258. [PubMed: 1878461]
19. Gris D, Marsh DR, Oatway MA, Chen Y, Hamilton EF, Dekaban GA, Weaver LC. Transient blockade of the CD11d/CD 18 integrin reduces secondary damage after spinal cord injury, improving sensory, autonomic, and motor function. J Neurosci. 2004; 24(16):4043–4051. [PubMed: 15102919]
20. Gris P, Tighe A, Thawer S, Hemphill A, Oatway M, Weaver L, Dekaban GA, Brown A. Gene expression profiling in anti-CD11d mAb-treated spinal cord-injured rats. J Neuroimmunol. 2009; 209(1–2):104–113. [PubMed: 19250688]
21. Hakamata Y, Tahara K, Uchida H, Sakuma Y, Nakamura M, Kume A, Murakami T, Takahashi M, Takahashi R, Hirabayashi M, Ueda M, Miyoshi I, Kasai N, Kobayashi E. Green fluorescent protein-transgenic rat: A tool for organ transplantation research. Biochem Biophys Res Commun. 2001; 286(4):779–785. [PubMed: 11520065]
22. Hermanns S, Reiprich P, Muller HW. A reliable method to reduce collagen scar formation in the lesioned rat spinal cord. J Neurosci Methods. 2001; 110(1–2):141–146. [PubMed: 11564534]
23. Hill CE, Moon LD, Wood PM, Bunge MB. Labeled Schwann cell transplantation: Cell loss, host Schwann cell replacement, and strategies to enhance survival. Glia. 2006; 53(3):338–343. [PubMed: 16267833]
24. Himes BT, Neuhuber B, Coleman C, Kushner R, Swanger SA, Kopen GC, Wagner J, Shumsky JS, Fischer I. Recovery of function following grafting of human bone marrow-derived stromal cells into the injured spinal cord. Neurorehabil Neural Repair. 2006; 20(2):278–296. [PubMed: 16679505]
25. Hofstetter CP, Schwarz EJ, Hess D, Widenfalk J, El Manira A, Prockop DJ, Olson L. Marrow stromal cells form guiding strands in the injured spinal cord and promote recovery. Proc Natl Acad Sci USA. 2002; 99(4):2199–2204. [PubMed: 11854516]
26. Huang WC, Kuo WC, Cherng JH, Hsu SH, Chen PR, Huang SH, Huang MC, Liu JC, Cheng H. Chondroitinase ABC promotes axonal regrowth and behavior recovery in spinal cord injury. Biochem Biophys Res Commun. 2006; 349(3):963–968. [PubMed: 16965762]
27. Inman DM, Steward O. Ascending sensory, but not other long-tract axons, regenerate into the connective tissue matrix that forms at the site of a spinal cord injury in mice. J Comp Neurol. 2003; 462(4):431–449. [PubMed: 12811811]
28. Inman DM, Steward O. Physical size does not determine the unique histopathological response seen in the injured mouse spinal cord. J Neurotrauma. 2003; 20(1):33–42. [PubMed: 12614586]
29. Jacob JE, Gris P, Fehlings MG, Weaver LC, Brown A. Autonomic dysreflexia after spinal cord transection or compression in 129Sv, C57BL, and Wallerian degeneration slow mutant mice. Exp Neurol. 2003; 183(1):136–146. [PubMed: 12957497]
30. Jacob JE, Pniak A, Weaver LC, Brown A. Autonomic dysreflexia in a mouse model of spinal cord injury. Neuroscience. 2001; 108(4):687–693. [PubMed: 11738503]
31. Jones LL, Sajed D, Tuszynski MH. Axonal regeneration through regions of chondroitin sulfate proteoglycan deposition after spinal cord injury: A balance of permissiveness and inhibition. J Neurosci. 2003; 23(28):9276–9288. [PubMed: 14561854]
32. Joshi M, Fehlings MG. Development and characterization of a novel, graded model of clip compressive spinal cord injury in the mouse: Part 1. Clip design, behavioral outcomes, and histopathology. J Neurotrauma. 2002; 19(2):175–190. [PubMed: 11893021]
33. Kigerl KA, McGaughy VM, Popovich PG. Comparative analysis of lesion development and intraspinal inflammation in four strains of mice following spinal contusion injury. J Comp Neurol. 2006; 494(4):578–594. [PubMed: 16374800]

34. Koda M, Okada S, Nakayama T, Koshizuka S, Kamada T, Nishio Y, Someya Y, Yoshinaga K, Okawa A, Moriya H, Yamazaki M. Hematopoietic stem cell and marrow stromal cell for spinal cord injury in mice. Neuroreport. 2005; 16(16):1763–1767. [PubMed: 16237323]
35. Lu P, Jones LL, Tuszynski MH. Axon regeneration through scars and into sites of chronic spinal cord injury. Exp Neurol. 2007; 203(1):8–21. [PubMed: 17014846]
36. Lu P, Jones LL, Tuszynski MH. BDNF-expressing marrow stromal cells support extensive axonal growth at sites of spinal cord injury. Exp Neurol. 2005; 191(2):344–360. [PubMed: 15649491]
37. Ma M, Basso DM, Walters P, Stokes BT, Jakeman LB. Behavioral and histological outcomes following graded spinal cord contusion injury in the C57B1/6 mouse. Exp Neurol. 2001; 169(2): 239–254. [PubMed: 11358439]
38. Morris RJ, Liu Y, Maries L, Yang Z, Trempus C, Li S, Lin JS, Sawicki JA, Cotsarelis G. Capturing and profiling adult hair follicle stem cells. Nat Biotechnol. 2004; 22(4):411–417. [PubMed: 15024388]
39. Nauta AJ, Fibbe WE. Immunomodulatory properties of mesenchymal stromal cells. Blood. 2007; 110(10):3499–3506. [PubMed: 17664353]
40. Neuhuber B, Timothy Himes B, Shumsky JS, Gallo G, Fischer I. Axon growth and recovery of function supported by human bone marrow stromal cells in the injured spinal cord exhibit donor variations. Brain Res. 2005; 1035(1):73–85. [PubMed: 15713279]
41. Ohta M, Suzuki Y, Noda T, Ejiri Y, Dezawa M, Kataoka K, Chou H, Ishikawa N, Matsumoto N, Iwashita Y, Mizuta E, Kuno S, Ide C. Bone marrow stromal cells infused into the cerebrospinal fluid promote functional recovery of the injured rat spinal cord with reduced cavity formation. Exp Neurol. 2004; 187(2):266–278. [PubMed: 15144853]
42. Okada S, Nakamura M, Mikami Y, Shimazaki T, Mihara M, Ohsugi Y, Iwamoto Y, Yoshizaki K, Kishimoto T, Toyama Y, Okano H. Blockade of interleukin-6 receptor suppresses reactive astrogliosis and ameliorates functional recovery in experimental spinal cord injury. J Neurosci Res. 2004; 76(2):265–276. [PubMed: 15048924]
43. Popovich PG, Guan Z, Wei P, Huitinga I, van Rooijen N, Stokes BT. Depletion of hematogenous macrophages promotes partial hindlimb recovery and neuroanatomical repair after experimental spinal cord injury. Exp Neurol. 1999; 158(2):351–365. [PubMed: 10415142]
44. Saruhashi Y, Young W, Perkins R. The recovery of 5-HT immunoreactivity in lumbosacral spinal cord and locomotor function after thoracic hemisection. Exp Neurol. 1996; 139(2):203–213. [PubMed: 8654523]
45. Saville LR, Pospisil CH, Mawhinney LA, Bao F, Simedrea FC, Peters AA, O'Connell PJ, Weaver LC, Dekaban GA. A monoclonal antibody to CD11d reduces the inflammatory infiltrate into the injured spinal cord: A potential neuroprotective treatment. J Neuroimmunol. 2004; 156(1–2):42–57. [PubMed: 15465595]
46. Sheth RN, Manzano G, Li X, Levi AD. Transplantation of human bone marrow-derived stromal cells into the contused spinal cord of nude rats. J Neurosurg Spine. 2008; 8(2):153–162. [PubMed: 18248287]
47. Siegel G, Schafer R, Dazzi F. The immunosuppressive properties of mesenchymal stem cells. Transplantation. 2009; 87(9 Suppl):S45–49. [PubMed: 19424005]
48. Stichel CC, Hermanns S, Luhmann HJ, Lausberg F, Niermann H, D'Urso D, Servos G, Hartwig HG, Muller HW. Inhibition of collagen IV deposition promotes regeneration of injured CNS axons. Eur J Neurosci. 1999; 11(2):632–646. [PubMed: 10051764]
49. Takami T, Oudega M, Bates ML, Wood PM, Kleitman N, Bunge MB. Schwann cell but not olfactory ensheathing glia transplants improve hindlimb locomotor performance in the moderately contused adult rat thoracic spinal cord. J Neurosci. 2002; 22(15):6670–6681. [PubMed: 12151546]
50. Tetzlaff W, Okon EB, Karimi-Abdolrezaee S, Hill CE, Sparling JS, Plemel JR, Plunet W, Tsai E, Baptiste DC, Smithson LJ, Kawaja MD, Fehlings M, Kwon BK. A systematic review of cellular transplantation therapies for spinal cord injury. J Neurotrauma. 2010; 72:1–72.
51. Tom VJ, Doller CM, Malouf AT, Silver J. Astrocyte-associated fibronectin is critical for axonal regeneration in adult white matter. J Neurosci. 2004; 24(42):9282–9290. [PubMed: 15496664]
52. Torrente Y, Polli E. Mesenchymal stem cell transplantation for neurodegenerative diseases. Cell Transplant. 2008; 17(10–11):1103–1113. [PubMed: 19181205]

53. Uccelli A, Moretta L, Pistoia V. Mesenchymal stem cells in health and disease. Nat Rev Immunol. 2008; 8(9):726–736. [PubMed: 19172693]
54. Vaquero J, Zurita M, Oya S, Santos M. Cell therapy using bone marrow stromal cells in chronic paraplegic rats: Systemic or local administration? Neurosci Lett. 2006; 398(1–2):129–134. [PubMed: 16423458]
55. Wiksten M, Vaananen AJ, Liebkind R, Liesi P. Regeneration of adult rat spinal cord is promoted by the soluble KDI domain of gammal laminin. J Neurosci Res. 2004; 78(3):403–410. [PubMed: 15468336]
56. Wu S, Suzuki Y, Ejiri Y, Noda T, Bai H, Kitada M, Kataoka K, Ohta M, Chou R, Ide C. Bone marrow stromal cells enhance differentiation of cocultured neurosphere cells and promote regeneration of injured spinal cord. J Neurosci Res. 2003; 72(3):343–351. [PubMed: 12692901]
57. Zhang Q, Shi S, Liu Y, Uyanne J, Shi Y, Le AD. Mesenchymal stem cells derived from human gingiva are capable of immunomodulatory functions and ameliorate inflammation-related tissue destruction in experimental colitis. J Immunol. 2009; 183(12):7787–7798. [PubMed: 19923445]
58. Zurita M, Vaquero J. Bone marrow stromal cells can achieve cure of chronic paraplegic rats: Functional and morphological outcome one year after transplantation. Neurosci Lett. 2006; 402(1–2):51–56. [PubMed: 16713677]
59. Zurita M, Vaquero J. Functional recovery in chronic paraplegia after bone marrow stromal cells transplantation. Neuroreport. 2004; 15(7):1105–1108. [PubMed: 15129154]
60. Zurita M, Vaquero J, Oya S, Miguel M. Schwann cells induce neuronal differentiation of bone marrow stromal cells. Neuroreport. 2005; 16(5):505–508. [PubMed: 15770160]

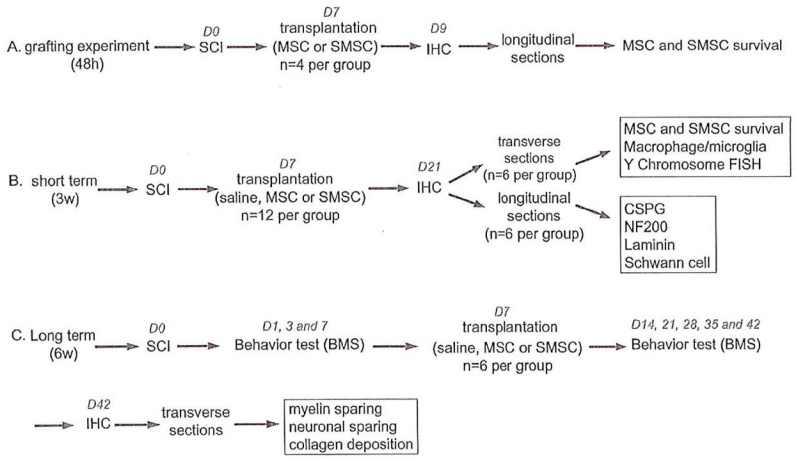

Figure 1.

Experimental design. (A) Eight Kr15-EGFP mice underwent SCI and then 7 days later were selected to receive either MSC or SMSC grafts (n = 4 per group). Forty-eight hours posttransplantation, all mice were sacrificed by cardiac perfusion and their spinal cord was sectioned for anti-GFP staining. (B) Thirty-six mice underwent SCI and then 7 days later were selected to receive either saline or MSC or SMSC grafts (n = 12 per group). Mice were subsequently sacrificed by cardiac perfusion and their spinal cord prepared for histological investigations as indicated. (C) Eighteen mice underwent SCI and received either saline or MSC or SMSC grafts (n = 6 per group) 7 days post-SCI. All mice were evaluated at 1, 3, 7, 10, 14, 21, 28, 35, and 42 days postinjury for locomotor recovery. Mice were subsequently sacrificed by cardiac perfusion and their spinal cord prepared for histological investigations as indicated.

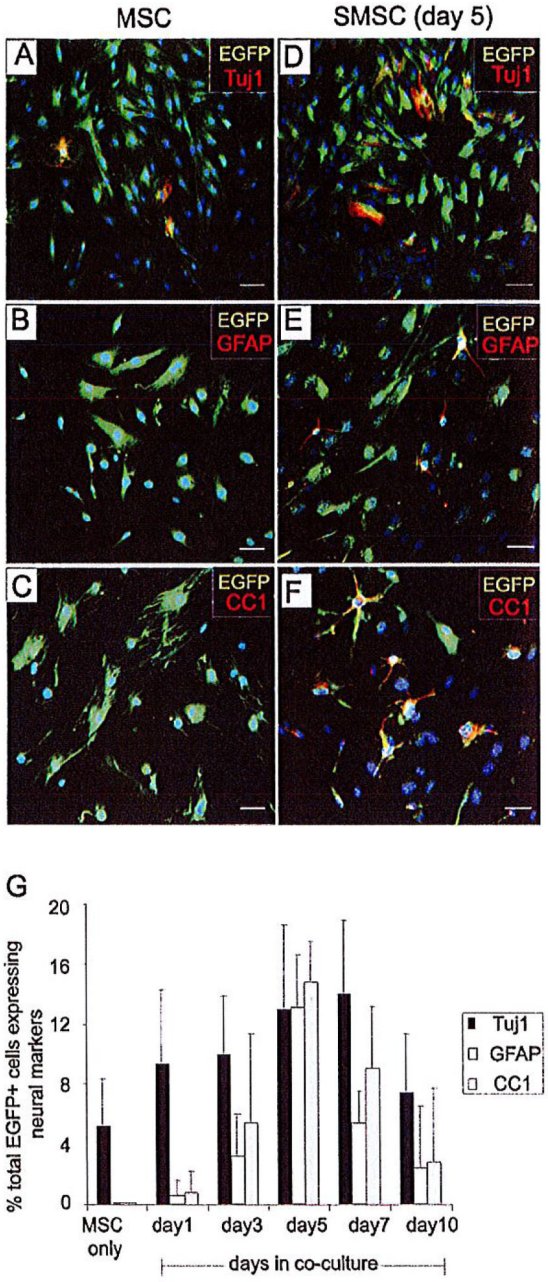

Figure 2.

MSCs express neural-specific markers after coculturing with Schwann cells. (A) A small percentage of MSCs cultured alone expressed the neuronal marker Tuj1, but did not express the astrocyte marker GFAP (B) or the oligodendrocyte marker CC1 (C). The percentage of MSCs positive for Tuj1 (D), GFAP (E), and CC1 (F) was increased after coculturing with Schwann cells for 5 days. (G) Quantification of neural markers expressed by $EGFP^+$ MSCs before and after coculturing with Schwann cells for 1–10 days ($n = 3$). Scale bars: 100 μm.

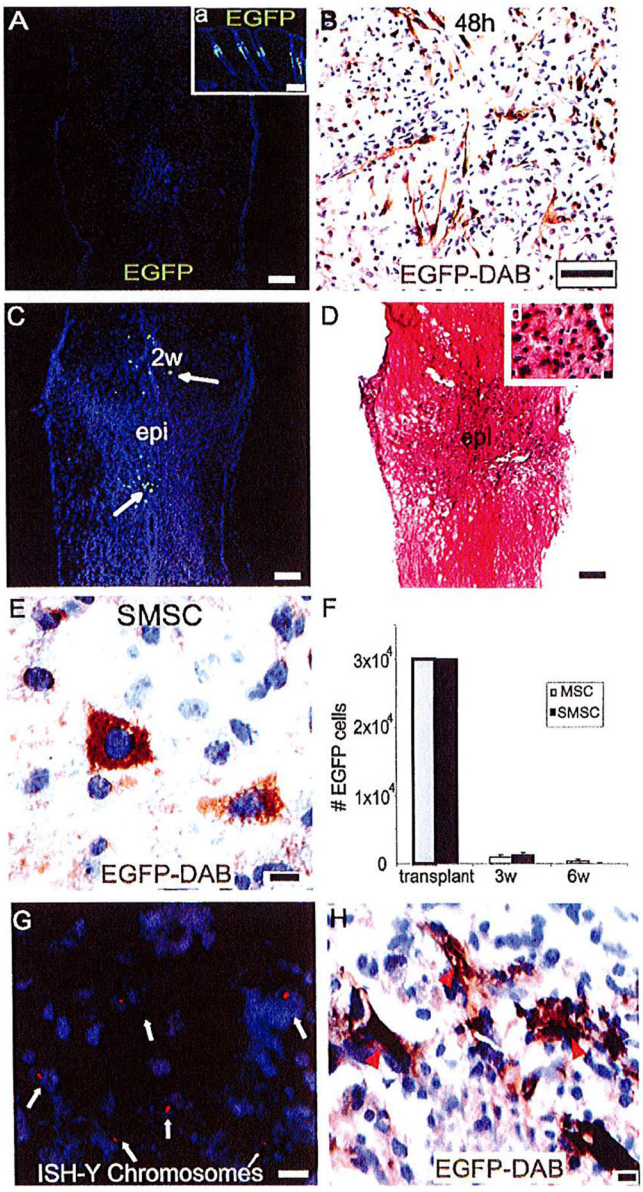

Figure 3.

MSCs and SMSCs survive temporarily in the injured spinal cord. (A) EGFP$^+$ cells were not found in the injured spinal cord of Kr15-EGFP control mice, whereas robust EGFP expression was demonstrated in skin hair follicles (inset) of the injured Kr15-EGFP mice. (B) EGFP$^+$ MSCs and SMSCs were readily found in the injured cord 48 h posttransplantation. EGFP$^+$ transplanted MSCs and SMSCs were located at the interface between the spared neural tissue and the lesion 3 weeks after transplantation (C–E), while the lesion epicenter was filled with inflammatory cells [(D), and high magnification inset d; the epicenter is indicated by “epi,” rostral is up]. (F) Approximately 3% and 1% of transplanted EGFP$^+$ cells survived until 3 and 6 weeks after transplantation, respectively. (G) Y chromosome in situ hybridization demonstrates the presence of a few transplanted Y chromosome-reactive MSCs per section (white arrows) in spinal cord sections taken from

the penumbral region (not the lesion epicenter) of a female recipient of transplanted MSCs 3 weeks after SCI. High magnification inset clearly shows the Y chromosome probe signal (red) in the DAPI (blue)-stained nuclei. (H) A directly adjacent serial section immunostained with an anti-GFP antibody demonstrates a few GFP-expressing MSCs (arrowheads) in the same location of the injured cord. *Statistically significant difference, $p < 0.05$ versus day 0. Scale bars: 100 μm (A–D, inset a); 10 μm (inset d, E, G, H).

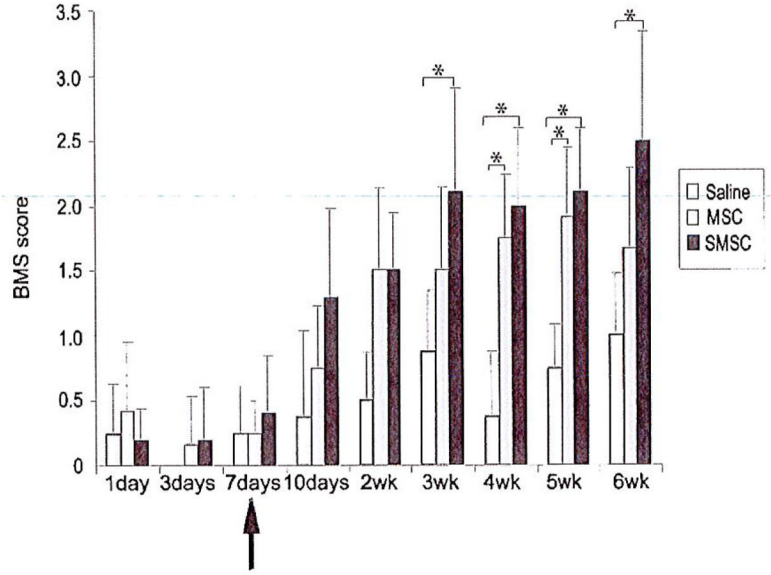

Figure 4.

MSC and SMSC transplants improve functional recovery after SCI. Recovery of locomotor function was evaluated using the 9-point Basso mouse scale (BMS). Arrow indicates administration of either saline, MSCs, or SMSCs 7 days after SCI. MSC- or SMSC-treated mice demonstrated significant improvement in locomotor function, compared to saline control mice, starting at 3 weeks postinjury for SMSC-treated mice and at 4 weeks postinjury for MSC-treated mice. *Statistically significant difference, $p < 0.05$, Neuman-Keuls posttest ($n = 6$ per group).

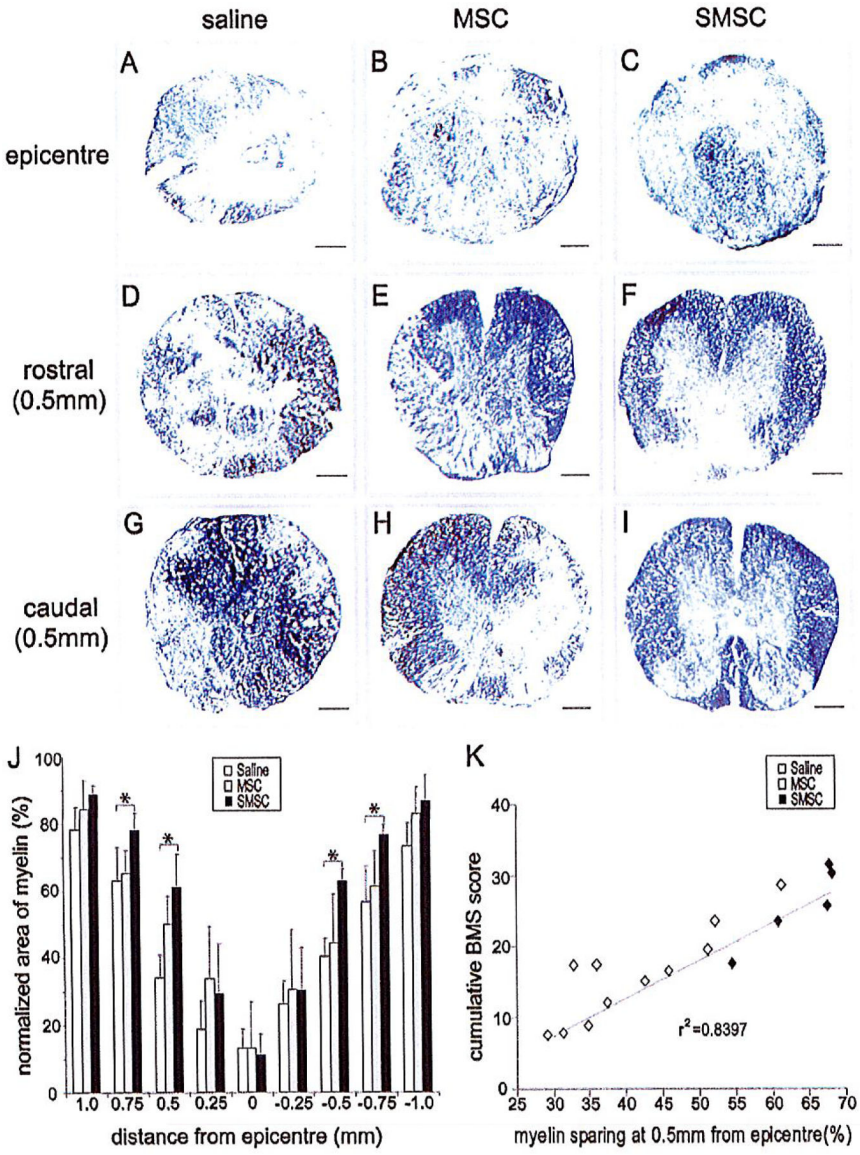

Figure 5.

SMSC transplants increase spared myelin 6 weeks after SCI. (A–I) Representative examples of solochrome cyanin-stained sections are shown at the lesion epicenter (A–C), at 0.5 mm rostral (D–F) and 0.5 mm caudal (G–I) to the epicenter, in saline control and MSC- and SMSC-treated mice. Dorsal is up. Scale bars: 100 μm. The area of blue-stained myelin was statistically greater in SMSC-treated mice than in controls at 0.5 and 0.75 mm rostral and caudal to the lesion epicenter. (J) Graphical representation illustrates the treatment effects on normalized area of compact myelin after SCI ($n = 6$ for saline group, $n = 5$ for MSC- and SMSC-treated groups). The zero point represents the lesion epicenter; positive positions are rostral and negative positions are caudal to the epicenter. *Statistically significant difference, $p < 0.05$, Neuman-Keuls posttest. (K) Correlation between functional outcome (cumulative BMS scores) and myelin sparing. The cumulative BMS scores of individual animals were

plotted as a function of the percentage of the averaged myelin sparing at 0.5 mm rostral and caudal to the epicenter.

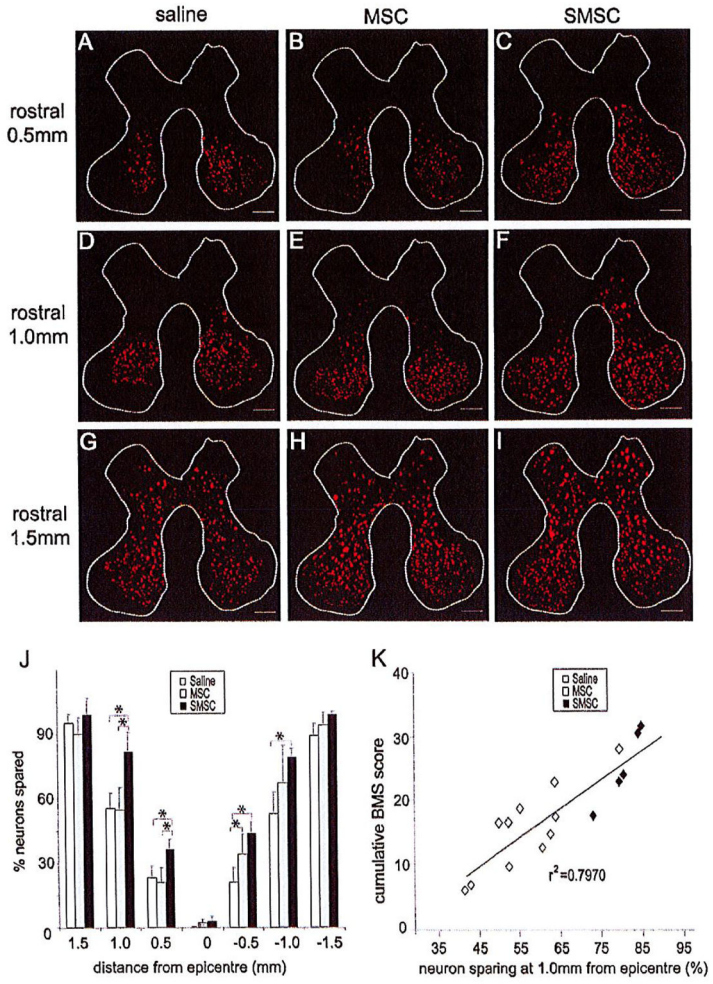

Figure 6.

Neuronal sparing 6 weeks after SCI. (A–I) Representative examples of NeuN$^+$ immunohistochemistry are shown at 0.5 mm (A–C), 1.0 mm (D–F), and 1.5 mm (G–I) rostral to the lesion epicenter, in saline-, MSC-, and SMSC-treated mice, respectively. Dorsal is up. Scale bars: 100 m. (J) The graph represents the average number of NeuN-immunoreactive neurons as a percentage to the total number of neurons from adjacent normal cord sections ($n = 6$ for saline group, $n = 5$ for MSC- and SMSC-treated groups). *Statistically significant difference, $p < 0.05$, Neuman-Keuls posttest. (K) Linear regression indicates a correlation between the cumulative BMS scores of individual animals and the averaged percentage of spared neurons at 1.0 mm rostral and 1.0 mm caudal to the epicenter.

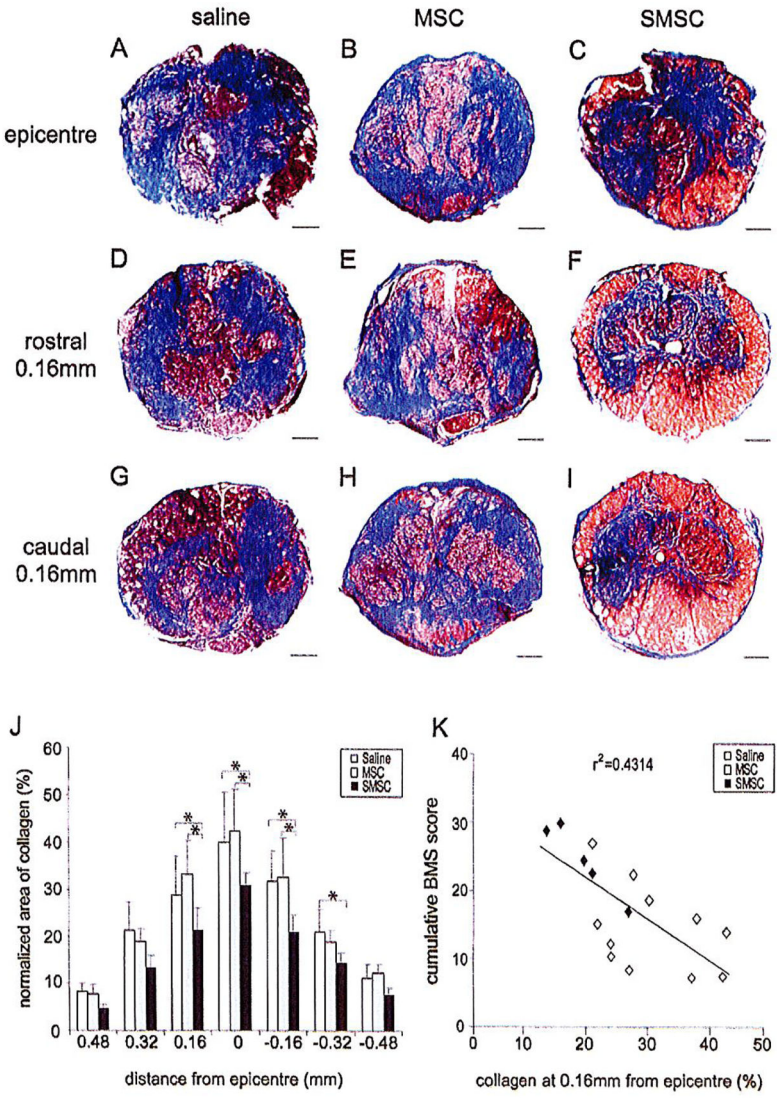

Figure 7.

SMSC transplants decrease the size of the collagen scar 6 weeks after SCI. (A–I) Masson's trichrome staining was performed to stain collagen at the lesion sites blue. Examples of trichrome-stained sections are shown at the lesion epicenter (A–C), at 0.16 mm rostral (D–F), and 0.16 mm caudal to epicenter (G–I), in saline controls and MSC- and SMSC-treated mice, respectively. Dorsal is up. Scale bars: 100 μm. (J) The graph demonstrates the calculated area of collagen as a percentage of the cross-sectional area of the same spinal cord section ($n = 6$ for saline group, $n = 5$ MSC- and SMSC-treated groups). *Statistically significant difference, $p < 0.05$, Neuman-Keuls posttest. (K) Linear regression indicates an inverse correlation between the cumulative BMS scores of individual animals and the averaged percent collagen area at 0.16 mm rostral and 0.16 mm caudal to the epicenter.

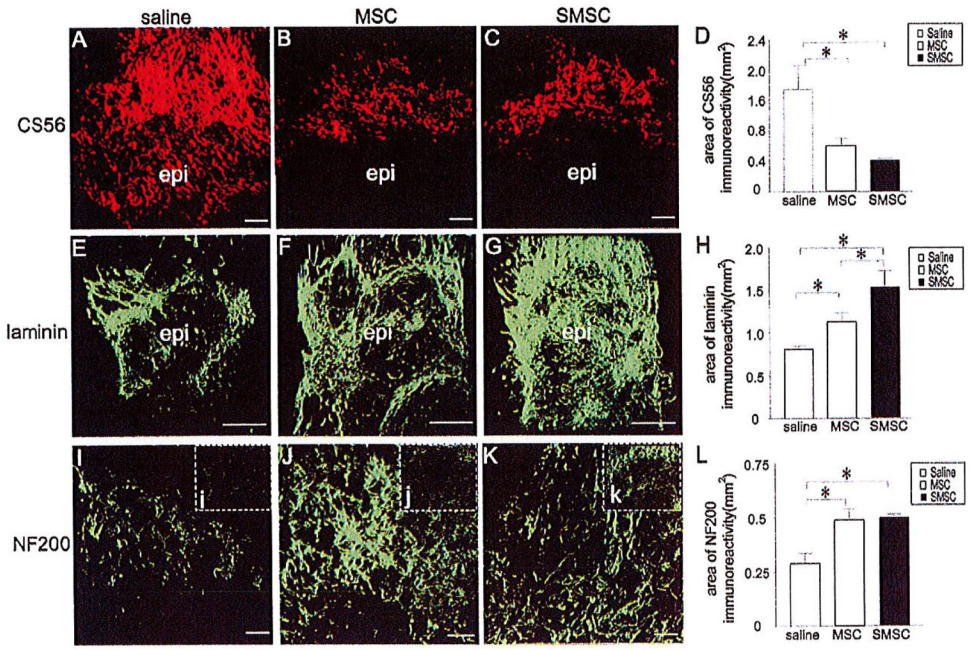

Figure 8.

MSC and SMSC transplantation alters scarring and wound healing after SCI. (A–C) CS56 immunoreactivity was mainly distributed in the penumbra adjacent to the lesion epicenter in saline controls (A) and MSC-treated (B) and SMSC-treated (C) mice (the position of the epicenter is outlined in white and rostral is up). (E–G) Extensive laminin immunoreactivity was observed in the penumbra, as well as at the lesion epicenter, in saline controls (E) and MSC-treated (F) and SMSC-treated (G) mice. (I–K) NF200 immunoreactivity was increased in the penumbra of MSC-treated (J) and SMSC-treated (K) mice compared to saline controls, (i–k) Insets demonstrate near total absence of NF200-labeled axons in the epicenter of the lesion in saline controls (i), and increased NF200-labeled axons in MSC-treated (j) and SMSC-treated mice (k). (D) The area of CS56 immunoreactivity was substantially reduced across the lesion in MSC-treated mice compared to saline controls. CS56 immunoreactivity was also reduced in SMSC-treated mice compared to both saline controls and MSC-treated mice. (H, L) The areas of laminin and NF200 immunoreactivity were increased in MSC- and SMSC-treated mice compared to saline controls. *Statistically significant difference, $p < 0.05$ ($n = 4$ for saline group; $n = 5$ for MSC and SMSC groups). Scale bars: 50 μm.

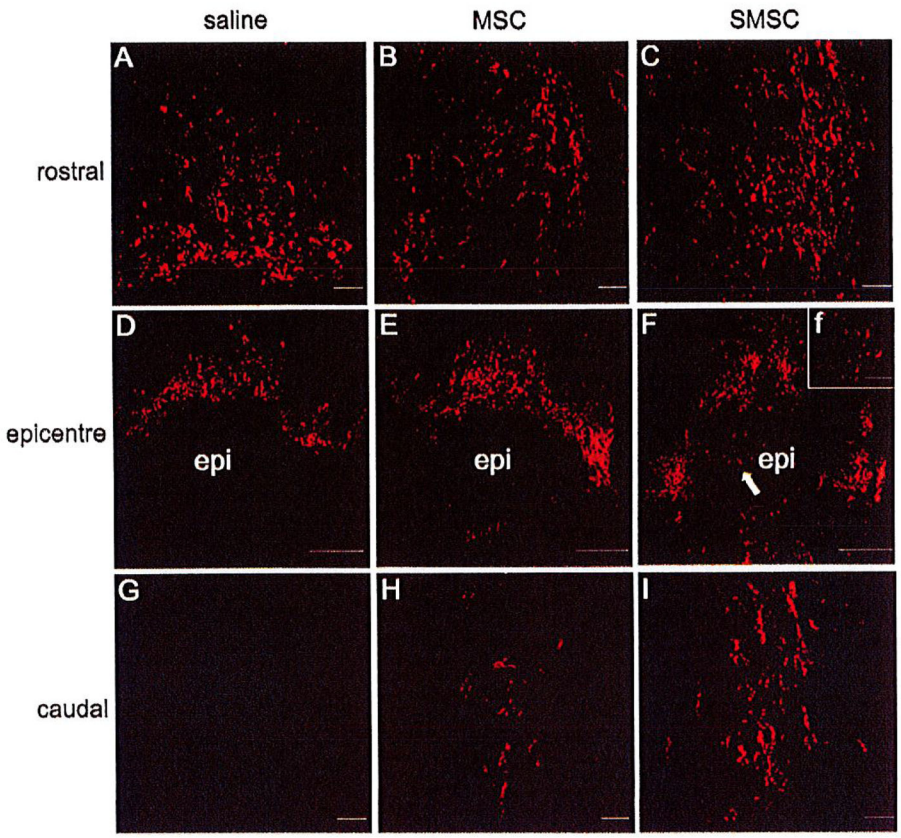

Figure 9.

MSCs and SMSCs increase serotonergic axons caudal to the lesion 2 weeks after transplantation. (A–C) 5-HT-positive axons accumulated rostral to the lesion epicenter in saline-treated (A), MSC-treated (B), and SMSC-treated mice (C). (D–F) 5-HT-positive fibers were not found at the lesion's edge in the saline control group (D), but were found at the edge of the lesion in MSC-treated (E) and SMSC-treated mice (F). 5-HT-positive axons were also observed in the epicenter of SMSC- but not MSC-treated mice (arrow in inset, f). (G–I) Caudal to the lesion, no 5-HT-positive fibers could be identified in saline controls (G) but were easily identified in MSC-treated (H) and SMSC-treated mice (I). Scale bar: 50 μm (A–C, G–I, f); 100 μm (D–F).

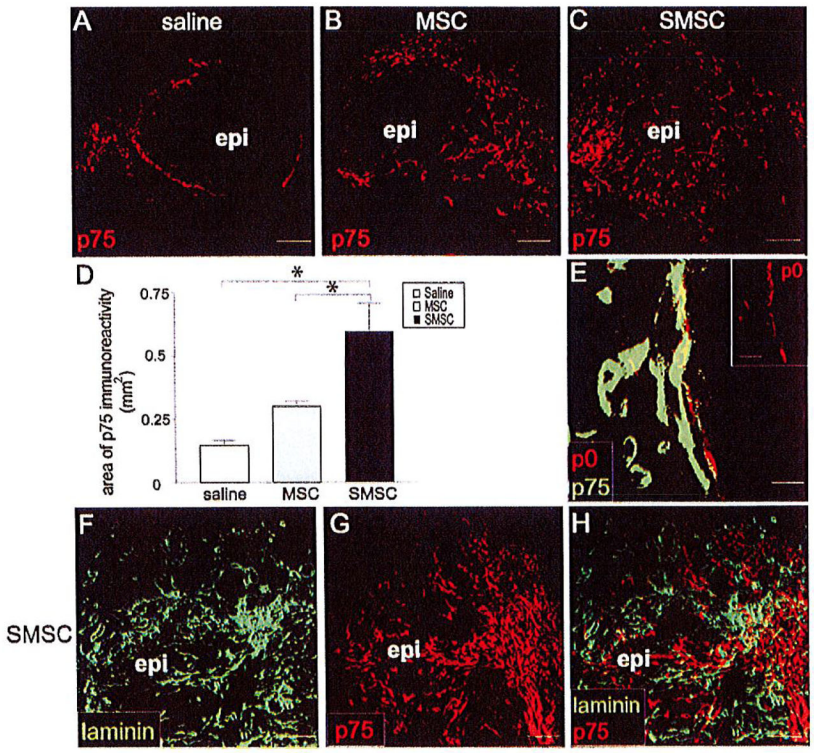

Figure 10.

MSCs and SMSCs increase Schwann cell infiltration of the lesion sites in mice 3 weeks after SCI. (A–C) p75-labeled Schwann cells were found in the lesion in all three groups. Very little p75 immunoreactivity was seen at the lesion epicenter in saline controls (A), whereas p75 immunoreactivity was present at the epicenter in MSC-treated (B) and SMSC-treated mice (C). (D) The graphical representation of the area of p75 immunoreactivity across the lesion suggests robust recruitment of Schwann cells after SMSC transplantation. The area of p75 immunoreactivity was significantly greater in SMSC-treated mice than in MSC-treated or control mice. (E) Confocal photomicrograph demonstrates colocalization of p75 and P0 immunoreactivity, suggesting that some Schwann cells participate in axon remyelination after SCI. (F–H) Representative photomicrographs demonstrating laminin and p75 immunoreactivity in the same areas of the lesion is serial sections, suggesting that Schwann cells may produce laminin. *Statistically significant difference, $p < 0.05$ ($n = 4$ for saline group; $n = 5$ for the MSC and SMSC groups). Scale barS: 100 μm (A–C), 5 μm (E), 50 μm (F–H).

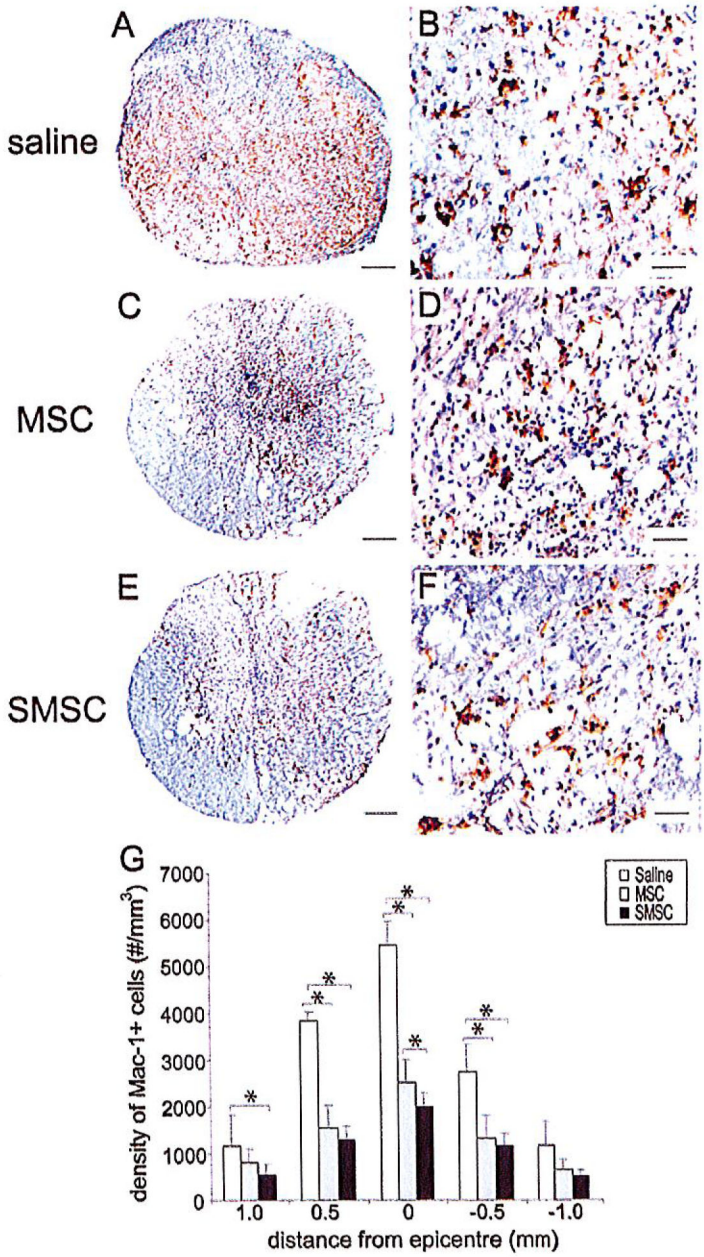

Figure 11.

Distribution of macrophages and active microglia at the lesion 3 weeks after SCI. (A–F) Representative examples of Mac-1-immunostained macrophages/microglia at the injury epicenter showing much lower density of Mac-1 labeling in MSC-treated (C, D) and SMSC-treated (E, F) mice compared to saline controls (A, B). (G) Graphical representation demonstrates that the number of Mac-1^+ cells decreased with distance from the epicenters and that the number of Mac-1^+ cells were substantially reduced in MSC- and SMSC-treated mice compared to saline controls. The density of Mac-1^+ cells was expressed as the number of Mac-1-expressing cells divided by the area of the section and multiplied by the thickness of the section (16 μm). *Statistically significant difference, $p < 0.05$, Neuman-Keuls posttest

(n = 3 for saline controls, n = 5 for MSC-treated group, and n = 6 for SMSC-treated group). Scale bars: 100 μm (A, C, E), 50 μm (B, D, F).

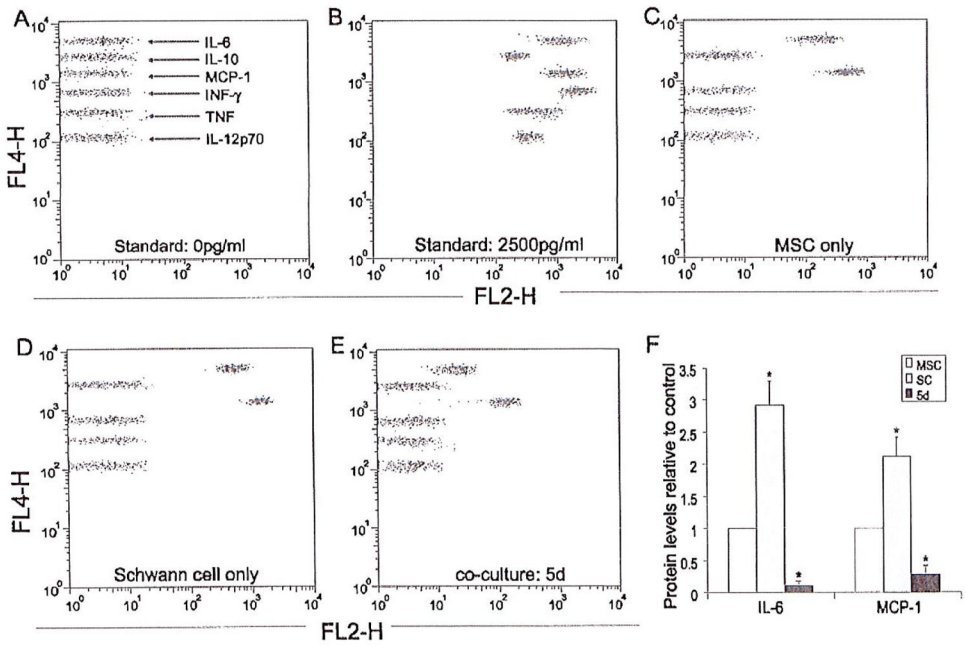

Figure 12.

MSC–Schwann cell cocultures produce less MCP-1 and IL-6 than MSC or Schwann cell cultures. Standard curves for each protein were created in each experiment ($n = 4$). Examples of negative control (A) and standard at 2500 pg/ml for each cytokine (B) were displayed as two-color dot plot (FL2 vs. FL4). Cytokine levels were determined in the supernatant collected from MSC culture (C), Schwann cell culture (D), and 5-day coculture (E). (F) The graph represents the concentrations of IL-6 and MCP-1 detected in the supernatant of MSC culture, Schwann cell culture, and 5-day coculture, normalized to the cytokine concentrations in MSC culture medium. *Statistically significant difference, $p < 0.05$ versus MSCs, Neuman-Keuls posttest.

Table 1

Summary of Tissue Sample Preparation

Experiment	Staining	Time (No. of Weeks Post-SCI)	No. of Sections per Animal	Section Orientation	Section Interval
MSC and SMSC grafting	anti-GFP	48 h	6	longitudinal	160 μm
MSC and SMSC survival	anti-GFP	3 and 6 weeks	25	transverse	32 μm
Myelin sparing	solochrome	6 weeks	9	transverse	250 μm
Collagen deposition	trichrome	6 weeks	7	transverse	160 μm
Neuronal sparing	anti-NeuN	6 weeks	39	transverse	80 μm
Macrophage density	anti-MAC-1	3 weeks	25	transverse	80 μm
CSPGs	anti-CS-56	3 weeks	4	longitudinal	32 μm
Neurofilament	anti-NF200	3 weeks	4	longitudinal	32 μm
Laminin	anti-laminin	3 weeks	4	longitudinal	32 μm
Schwann cells	anti-p75	3 weeks	4	longitudinal	32 μm

Table 2

List of Antibodies Used in Immunohistochemistry

Primary Antibody	Antigen	Secondary Antibody
Rabbit anti-EGFP (1:300; Invitrogen, Carlsbad, CA)	EGFP	Goat anti-rabbit IgG, Alexa Fluro (AF) 488 (1:1000; Molecular Probe, Carlsbad, CA), or Biotinylated donkey anti-rabbit IgG (1:200; Jackson ImmunoResearch, West Grove, PA), followed by avidin-peroxidase conjugate (Vector Laboratories, Burlingame, CA) and diaminobenzine (DAB, Zymed, Carlsbad, CA)
Mouse anti-β-III tubulin (Tuj1, 1:500; Chemicon, Temecula, CA)	β-III tubulin	Rat anti-mouse IgG, AF594 (1:1000; Molecular Probe)
Mouse anti-NeuN (1:300; Chemicon)	NeuN	Rat anti-mouse IgG, AF594 (1:1000; Molecular Probe)
Rabbit anti-GFAP (1:500; Calbiochem, La Jolla, CA)	GFAP	Goat anti-rabbit IgG, AF488 (1:1000; Molecular Probe)
Mouse anti-APC (CC1) (1:100; Calbiochem)	adenomatus polyposis coli (APC)	Rat anti-mouse IgG, AF594 (1:1000; Molecular Probe)
Anti-Mac-1 (CD11b, 1:600; DSHB, University of Iowa)	CD11b	Biotinylated goat anti-rat IgG (1:200; Jackson ImmunoResearch, West Grove, PA), followed by avidin-peroxidase conjugate (Vector Laboratories) and diaminobenzine (DAB, Zymed)
Mouse anti-CS-56 (1:300; Sigma, St. Louis, MO)	CSPG	Rat anti-mouse IgM (1:200; Invitrogen), followed by donkey anti-rat IgG, AF594 (1:1000; Molecular Probe)
Rabbit anti-NF200 (1:1000; Sigma)	NF200	Goat anti-rabbit IgG, AF488 (1:1000; Molecular Probe)
Rabbit anti-laminin (1:300; Sigma)	laminin	Goat anti-rabbit IgG, AF488 (1:1000; Molecular Probe)
Rabbit anti-p75 (1:150; Chemicon)	P75 nerve growth factor receptor	Goat anti-rabbit IgG, AF594 (1:1000; Molecular Probe)
Rabbit anti-5-HT (1:400; ImmunoStar, Hudson, WI)	5-HT	Goat anti-rabbit IgG, AF594 (1:1000; Molecular Probe)
Chicken anti-P0 (1:500; Aves Lab, Tigard, OR)	P0 myelin protein	Goat anti-chicken IgG, Cy5 (1:1000; Aves Lab)